Metadata of the chapter that will be visualized in SpringerLink

Book Title	Challenges and Innovations in Geomechanics
Series Title	
Chapter Title	PFEM Modeling of Strain Localization Processes in Non-local Multiplicative Plasticity
Copyright Year	2023
Copyright HolderName	The Author(s), under exclusive license to Springer Nature Switzerland AG

Corresponding Author	Family Name	**Oliynyk**
	Particle	
	Given Name	**Kateryna**
	Prefix	
	Suffix	
	Role	
	Division	School of Science and Engineering
	Organization	University of Dundee Nethergate
	Address	Dundee, D1 4HN, Scotland, UK
	Division	Department of Civil and Environmental Engineering
	Organization	University of Perugia
	Address	Via G. Duranti, 93, 06125, Perugia, Italy
	Email	2439697@dundee.ac.uk
Author	Family Name	**Ciantia**
	Particle	
	Given Name	**Matteo O.**
	Prefix	
	Suffix	
	Role	
	Division	School of Science and Engineering
	Organization	University of Dundee Nethergate
	Address	Dundee, D1 4HN, Scotland, UK
	Email	
Author	Family Name	**Tamagnini**
	Particle	
	Given Name	**Claudio**
	Prefix	
	Suffix	
	Role	
	Division	Department of Civil and Environmental Engineering
	Organization	University of Perugia
	Address	Via G. Duranti, 93, 06125, Perugia, Italy
	Email	

Abstract

A fully non-linear PFEM platform developed for coupled flow and deformation processes in saturated structured soils is employed in this work to explore the possibility of modeling the occurrence of strain localization and the evolution of the displacement field in the post-localization regime without the pathological mesh-dependence typically observed in conventional non-linear FEM simulation. The proposed formulation adopts an isotropic hardening elastoplastic model for bonded geomaterials, developed in the framework of multiplicative plasticity, equipped with non-local hardening laws of the integral type for both density- and bonding-related internal variables. These hardening laws provide the material with an internal length scale based on the size of the neighborhood where the non-local averaging is performed. A number of PFEM simulations of plane strain compression tests on ideal calcarenite specimens have been performed to explore the convergence of the numerical solution in the post-localization regime as the element size is reduced. The convergence study is focused on simulations with non-uniform, adaptive discretizations, exploring the convergence of the solution as the adopted minimum element size of the mesh is reduced. The results of the convergence study demonstrate the effectiveness of the adopted non-local approach in eliminating the pathological mesh-dependence in presence of strain localization, in the context of *h*-adaptive PFEM simulations.

Keywords (separated by '-')	PFEM - Strain localization - Non-local regularization - Finite deformation plasticity - Bonded soils

PFEM Modeling of Strain Localization Processes in Non-local Multiplicative Plasticity

Kateryna Oliynyk[1,2](✉), Matteo O. Ciantia[1], and Claudio Tamagnini[2]

[1] School of Science and Engineering, University of Dundee Nethergate, Dundee D1 4HN, Scotland, UK
2439697@dundee.ac.uk

[2] Department of Civil and Environmental Engineering, University of Perugia, Via G. Duranti, 93, 06125 Perugia, Italy

Abstract. A fully non-linear PFEM platform developed for coupled flow and deformation processes in saturated structured soils is employed in this work to explore the possibility of modeling the occurrence of strain localization and the evolution of the displacement field in the post-localization regime without the pathological mesh-dependence typically observed in conventional non-linear FEM simulation. The proposed formulation adopts an isotropic hardening elastoplastic model for bonded geomaterials, developed in the framework of multiplicative plasticity, equipped with non-local hardening laws of the integral type for both density- and bonding-related internal variables. These hardening laws provide the material with an internal length scale based on the size of the neighborhood where the non-local averaging is performed. A number of PFEM simulations of plane strain compression tests on ideal calcarenite specimens have been performed to explore the convergence of the numerical solution in the post-localization regime as the element size is reduced. The convergence study is focused on simulations with non-uniform, adaptive discretizations, exploring the convergence of the solution as the adopted minimum element size of the mesh is reduced. The results of the convergence study demonstrate the effectiveness of the adopted non-local approach in eliminating the pathological mesh-dependence in presence of strain localization, in the context of *h*-adaptive PFEM simulations.

Keywords: PFEM · Strain localization · Non-local regularization · Finite deformation plasticity · Bonded soils

1 Introduction

Strain localization in geomaterials is an almost ubiquitous phenomenon which can be observed at many different scales, from the laboratory specimen size to regional faults extending over hundreds of kilometers. Depending on the material properties, it may occur in a variety of forms: as concentrations of cracks; as distinct, planar frictional surfaces; as gouge zones of finely comminuted material; or simply as regions of concentrated shear strains. In granular materials, intense deviatoric deformations may be accompanied by dilation (inelastic volume increase) or compaction (inelastic volume

M. Barla et al. (Eds.): IACMAG 2022, LNCE 288, pp. 1–8, 2023.
https://doi.org/10.1007/978-3-031-12851-6_15

decrease) as well as by chemical alteration under large stress levels and high temperatures. Collapse of geotechnical structures is often characterized by the formation and propagation of zones of localized shear deformations. In such cases, the analysis of the conditions which lead to localized failure, as well as the study of the post-failure evolution of the system is of great importance in geotechnical engineering, and also in related disciplines such as earthquake engineering, mining and petroleum engineering, structural geology and geophysics.

In this work, following Monforte et al (2019) and Oliynyk et al. (2021), a fully non-linear PFEM platform is employed in this work to explore the possibility of modeling the occurrence of strain localization and the evolution of the displacement field in the post-localization regime without the pathological mesh-dependence typically observed in conventional non-linear FEM simulation. The key point in the proposed numerical approach is the adoption of an isotropic hardening elastoplastic model to describe the mechanical behavior of bonded geomaterials – the FD_Milan Model – equipped with non-local hardening laws. These hardening laws provide the material with an internal length scale based on the size of the neighborhood where the non-local averaging is performed. The PFEM code is then used to simulate a series of plane-strain compression tests on a soft rock with properties similar to those of Apulian calcarenites.

2 The FD_Milan Model

The FD_Milan model is a non-associative, isotropic hardening finite-deformation plasticity model for structured soils and weak rocks, developed by Oliynyk et al. (2021) based on the multiplicative decomposition of the deformation gradient and on the adoption of a suitable free energy function to describe the elastic response of the material. The details of the model are not provided here for space reasons. The model is equipped with two scalar internal variables, P_s (*preconsolidation pressure*, which accounts for the hardening/softening effects due to volumetric and deviatoric plastic strains) and P_t (*bond strength*, which quantifies the effects of material fabric and bonding). A representation of the yield surface in the Kirchhoff stress invariants space $Q : P$, highlighting the role of the internal variables, is given in Fig. 1.

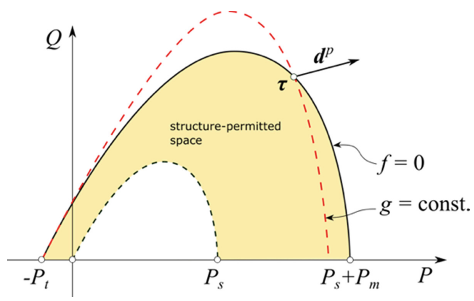

Fig. 1. Yield surface and plastic potential of the FD_Milan model

A positive value of the bond strength P_t results in an expansion of the elastic domain in stress space. On the positive part of the P axis, the isotropic yield stress in compression is increased by a quantity $P_m = kP_t$, with k a material constant. On the negative axis, the vertex of the yield surface is displaced from the origin to $P = -P_t$. Therefore, the structured material possesses a true cohesion and a non-negligible tensile strength. The region in the stress space contained between the actual yield surface (full black line in Fig. 1) and the intrinsic yield surface of the unstructured material (with $P_t = P_m = 0$, black dashed line in the figure), represents the so-called *structure-permitted space*, which is accessible only by the combined effects of fabric and intergranular bonding. As a consequence of the microstructural rearrangement of the soil fabric and the concurrent breakage of intergranular bonds, the structure of the material is progressively destroyed. From a macroscopic point of view, this process induces a progressive reduction of P_t with increasing accumulated plastic deformations. This process is described by a suitable monotonic hardening law, yielding $P_t = 0$ as the asymptotic value for very large accumulated plastic deformations.

In order to provide a characteristic length scale to the constitutive equation, with the objective of regularizing the numerical solution in presence of strain localization, the integral non-local approach of Oliynyk et al. (2021) has been adopted, in which the internal variables are treated as non-local, spatially averaged quantities over a neighborhood Ω of the material point. The size of this neighborhood is controlled by a material constant l_c, called *characteristic length.*

3 PFEM Simulations of Plane Strain Compression Tests

A reference specimen with a width $B = 1.0$ m and an aspect ratio $H/B = 1.8$ has been considered in all the simulations. The displacements in direction z are fixed, and the specimen deforms under plane strain conditions, with prescribed vertical displacements on the top and bottom boundaries and prescribed normal surface tractions on the lateral boundaries. The self weight of the soil has been ignored by setting to zero the gravity acceleration, so that the actual dimensions of the specimen are not relevant. All the test have been performed under drained conditions, with $p_w = 0$. A vertical shortening u has been imposed at the top boundary in constant steps $\Delta u/H = 5.0\text{e}{-4}$, up to a final value of $u/H = 0.20$, while vertical displacements have been fixed at the bottom boundary. The horizontal displacements along the top and bottom boundaries have been kept either fixed, to simulate perfectly rough end platens, or free, to simulate perfectly smooth end platens. The material constants adopted in the simulations are provided in Table 1. This set of data, taken from Oliynyk et al. (2021), can be considered representative of a weak calcarenite rock.

In all the tests, the initial values of P_s and P_t have been assumed equal to -300 kPa and -200 kPa, respectively. The complete set of biaxial test simulations is given in Table 2.

The 6 simulations of Group 1 (r100–r105) have been performed to assess the convergence of the numerical solution in the post-localization regime as the element size is reduced. This allows to check the capability of the non-local formulation to avoid the pathological mesh dependence observed when local constitutive models with no internal length scale are used to simulate the spontaneous tendence of the deformation field to localize into narrow bands.

Table 1. Material constants for the FD_Milan model adopted in the simulations.

$\hat{\kappa}$ (−)	G_0 (MPa)	α (−)	P_{ref} (MPa)	$M_{f,c}$ (−)	α_f (−)	μ_f (−)	$M_{g,c}$ (−)
0.24	45.45	0.0	10.0	1.30	0.75	1.50	1.675
α_g (−)	μ_g (−)	ρ_s (−)	ρ_t (−)	ξ_s (−)	ξ_t (−)	k (−)	l_c (m)
0.01	1.20	20.0	15.0	0.0	0.5	5	Variable

Table 2. Program of numerical simulations**.**

Group1	r100	r101	r102	r103	r104	r105
p_0(MPa)	0.0	0.0	0.0	0.0	0.0	0.0
l_c/B	0.15	0.15	0.15	0.15	0.15	0.15
h_{crit}/l_c	0.07	0.10	0.33	0.50	0.10	0.67
Bases	Rough	Rough	Rough	Rough	Rough	Rough
Group 2	r200	r201	r202	r203	r204	r205
p_0(MPa)	0.0	0.0	0.0	0.0	0.0	0.0
l_c/B	0.10	0.15	0.30	0.10	0.15	0.30
h_{crit}/l_c	0.10	0.10	0.10	0.10	0.10	0.10
Bases	Rough	Rough	Rough	Smooth	Smooth	Smooth

Typically, convergence studies of this kind are performed by uniformly reducing the element size over the entire domain (see, e.g., Mánica et al. 2018). In this work, we addressed the convergence study towards simulations with non-uniform, adaptive discretizations, exploring the convergence of the solution as the minimum element size of the discretization is reduced. The reason for this choice is that adaptive remeshing is an essential component of PFEM algorithmic strategy as well as an essential feature to achieve a high computational efficiency in the solution of BVPs of practical interest. To this end, simulations r100 to r103 have been performed changing the ratio between the critical element size h_{crit} – which controls the minimum element size – and the characteristic length l_c of the material. For comparison, uniform discretizations have been adopted in the last two simulations of this group – fine for simulation r104 and coarse for simulation r105. All the simulations of Group 1 have been performed assuming zero confining pressure, perfectly rough end platens and a constant length $l_c = 0.15B$.

The 6 simulations of Group 2 have been performed with the aim of studying the effects of the chosen characteristic length l_c on the strain localization pattern, in terms of shear band inclination and thickness. Both rough and smooth end platens have been considered, to investigate the effects of the adopted boundary conditions on strain localization.

4 Results

The localization patterns typically observed in the simulations of both Group 1 and 2 are shown in Fig. 2, which reports the contour maps of accumulated plastic deviatoric deformation E_s^p for two representative simulations: r201, performed with perfectly rough end platens, and r204, performed with perfectly smooth end platens.

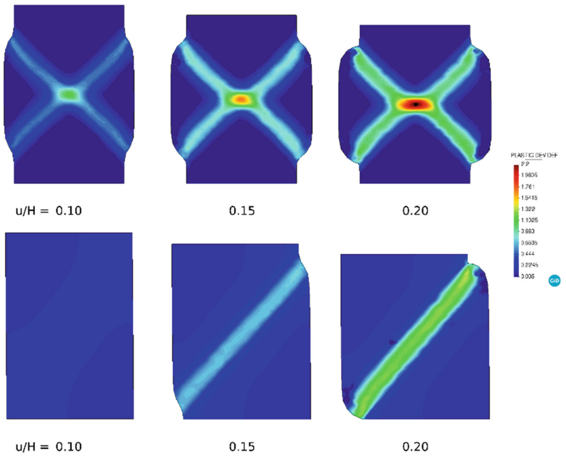

Fig. 2. Shear band geometry with increasing normalized shortening. Top row: simulation r201 with rough end platens. Bottom row: simulation r204 with smooth end platens

From the maps on the top line of Fig. 2, it is apparent that in simulation r200, as soon as the material starts to yield, the deformations inside the specimen localize in two conjugated shear bands, starting close to the rough specimen bases and meeting at the specimen center. In this case, the localization is triggered by the kinematic constraints imposed at the top and bottom platens. The two bands separate the specimen into four almost rigid wedges, two of which are attached to the loading platens. As u/H increases, the two central wedges are compressed at their vertex (at the center of the specimen), while the remaining two are displaced laterally. At significant vertical shortening, the alignment between the two portions of the initially planar bands is lost.

On the contrary, in simulation r204 the boundary conditions imposed at the top and bottom boundaries are compatible with a perfectly homogeneous solution. This solution is followed up to elongations $u/H \simeq 0.1$, after which strain localization appears as a consequence of the branch switching from the (less stable) homogeneous path to the (more stable) localized solution, as a consequence of some small inhomogenenities caused by numerical approximations, which are sufficient to trigger the onset of localization. In this case, the pattern of localized deformations is quite different from the one observed in simulation r201, with a single band of approximately the same inclination, running from the bottom left to the top right side of the specimen.

As far as the results of Group 1 simulations are concerned, Fig. 3 reports the evolution of the resultant force at the top platen divided by the reference specimen width, F/B, with increasing relative vertical shortening of the specimen, u/H, for different h_{crit}/l_c ratios in the range [0.07, 0.50]. All the simulations have reached the prescribed maximum shortening of 20% of the initial specimen height H. As expected for a highly cemented material loaded with no confining stress, the load-displacement response is brittle, with a strong strength reduction after the peak load is reached. The load-displacement curves of Fig. 3 do not represent the constitutive response of the material, since the stress and deformation fields are not homogeneous inside the specimen.

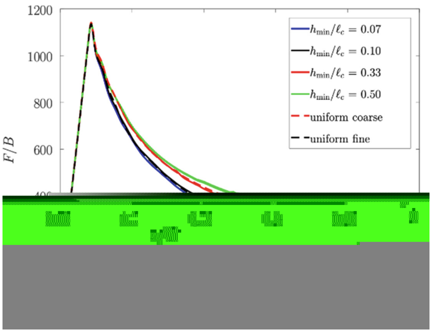

Fig. 3. Load-displacement curves for different values of h_{crit}/l_c

In all the simulations performed with adaptive remeshing, the predicted post-peak behavior is significantly affected by the evolving spatial discretization, the minimum element size of which is controlled by the ratio h_{crit}/l_c. From the examination of the final discretizations, it is apparent that the reason for the observed differences in the post peak response is to be found in the inability of the discretization to properly describe the strain localization process. However, as h_{crit}/l_c decreases and the remeshing algorithm captures the shear bands with a sufficient number of small elements, the distance between the different load-displacement curves reduces and convergence can be considered practically achieved for $h_{\text{crit}}/l_c = 0.1$. The results obtained with adaptive remeshing are also consistent with those provided by adopting a uniform fine mesh (simulation r104).

To detect as accurately as possible the geometric features of the localized deformation zones, the results of the simulations of Group 2 have been analyzed plotting the contours of the accumulated plastic deviatoric deformation E_s^p with very small upper and lower limits, as in Fig. 4 (relative to test r200). This has allowed to draw the band limits quite sharply, and to visually detect their orientation (red line in the figure), their inclination and the orientation of the normal to the band (black line in the figure).

For the evaluation of the band inclination θ, a line has been drawn which approximates as closely as possible the centerline of the upper portion of the descending band, as shown in Fig. 4. Then the computed values of E_s^p have been extracted along the normal to the band centerline and plotted *vs.* the distance ξ from the centerline (see Fig. 5) for different axial shortening values u/H. From the plots in Fig. 5, showing the results obtained from simulations r200 and r202, it is apparent that the definition of the band thickness b is somehow subjective. In order to define a conventional measure for b, a limiting threshold for E_s^p has been defined and the band limits have been fixed as the two points where the accumulated deviatoric plastic strain exceeds the threshold from the left ($\xi < 0$ and increasing) and from the right ($\xi > 0$ and decreasing).

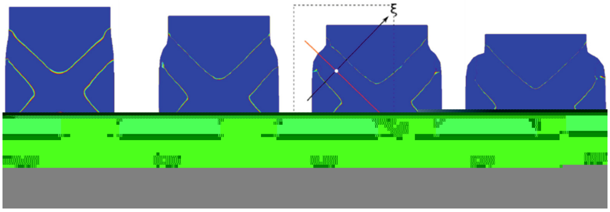

Fig. 4. Biaxial tests r200: localized deformation band contours at different values of u/H. The symbols θ and ξ indicate the band inclination and the distance from the band center along the normal to the band

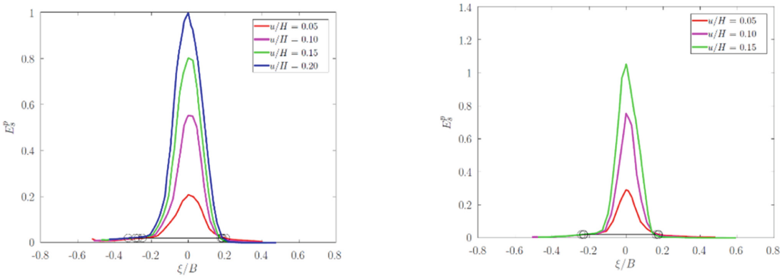

(a) (b)

Fig. 5. Profiles of accumulated plastic deviatoric strain E_s^p across the band, at different values of normalized shortening: a) simulation r200; b) simulation r202. The points on each curve indicate the conventional limits of the band.

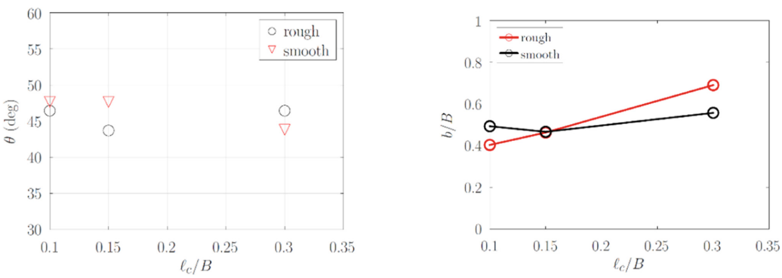

(a) (b)

Fig. 6. Results of simulations of Group 2: a) shear band inclination; b) normalized shear band width.

For consistency among the different simulations, the values of band inclination θ and of the band thickness b have been determined at a relative shortening $u/H = 0.15$, and a threshold value $E^p_{s,\mathrm{thr}} = 0.02$ has been adopted to identify the band limits.

The values of θ and b/B obtained in the simulations of Group 2 are plotted as a function of the characteristic length l_c in Fig. 6. The data on the measured band inclination appear rather scattered in a range between 43° and 47°, probably as a consequence of the particular method employed to measure θ, which implies a certain amount of subjectivity. The data do not provide any clear indication of a dependency of the band inclination on the characteristic length. On the contrary, as the characteristic length increases, the band width appears to increase almost linearly with l_c. This result is not confirmed by the simulations with smooth end platens, although some small increment of b is observed passing from $l_c/B = 0.15$ to 0.30.

5 Concluding Remarks

The numerical platform proposed in this work has proven to be very effective in dealing with strain localization phenomena. The results of the convergence study performed on the biaxial test simulations have demonstrated the effectiveness of the adopted non-local approach in eliminating the pathological mesh dependence of conventional FE simulations when using constitutive models lacking an internal length scale, in the context of *h*-adaptive PFEM simulations. As long as the minimum element size is sufficiently smaller than the shear band width, mesh refinement does not affect the final solution. This implies that objective results for large scale simulations can be obtained starting from an initially coarse discretization, with a significant saving in terms of computational costs. The characteristic length l_c seems to have a limited influence on the band orientation, while it controls the thickness of the localized zone in the simulations with rough boundaries. Additional work is required to clarify its role in situations such as the tests performed with smooth end platens, where the onset of localization is not occurring simultaneously with first plastic yielding.

Acknowledgements. The financial support of grant "Modeling of cemented soils and weak rocks subjected to destructuration and weathering" of the University of Perugia (DICA) is gratefully acknowledged.

References

Monforte, L., Ciantia, M.O., Carbonell, J.M., Arroyo, M., Gens, A.: A stable mesh-independent approach for numerical modelling of structured soils at large strains. Comput. Geotech. **116**, 103215 (2019)

Mánica, M.A., Gens, A., Vaunat, J., Ruiz, D.F.: Nonlocal plasticity modelling of strain localisation in stiff clays. Comput. Geotech. **103**, 138–150 (2018)

Oliynyk, K., Ciantia, M.O., Tamagnini, C.: A finite deformation multiplicative plasticity model with non – local hardening for bonded geomaterials. Comput. Geotech. **137** (2021)